Submitted: 06 January, 2023 Accepted: 02 February, 2023 Online Published: 28 February, 2023 DOI:10.22514/jomh.2023.013

ORIGINAL RESEARCH

JOMH Journal of Men's Health

Identification of a 6-gene signature associated with ferroptosis for predicting the prognosis in prostate cancer

Jing-jing Guan[1], Zhou-min Pan[2], Guan-an Zhao[3,*]

[1]Department of Pharmacy, Lishui City People's Hospital, 323000 Lishui, Zhejiang, China
[2]Endoscopy Center, Longquan People's Hospital, 323700 Lishui, Zhejiang, China
[3]Department of Urology, Lishui City People's Hospital, 323000 Lishui, Zhejiang, China

***Correspondence**
lyzhaoguanan@163.com
(Guan-an Zhao)

Abstract

Ferroptosis is intimately correlated with the development of cancers. We aimed to identify ferroptosis-related prognostic signatures for prognosis prediction of prostate adenocarcinoma (PRAD). The expression profile and clinical data of patients were from The Cancer Genome Atlas Program (TCGA) database. The Cox regression and Lasso analyses were utilized to construct a multigene signature, and the Kaplan-Meier (K-M), receiver operating characteristic (ROC), and decision curve analysis (DCA) curves were used to validate the predictive effect. Additionally, pathway enrichment analyses were performed to explore the potential mechanism associated with biomarkers. In this study, 41 ferroptosis-related genes (FRGs) were differentially expressed between PRAD and normal tissues. Then, we finally constructed a risk model consisting of 6 signatures (Transferrin Receptor (TFRC), Ferritin Heavy Chain 1 (FTH1), Poly (RC) Binding Protein 2 (PCBP2), Acyl-CoA Synthetase Long Chain Family Member 3 (ACSL3), Prion Protein (PRNP), and Lysophosphatidylcholine Acyltransferase 3 (LPCAT3)) among 41 biomarkers. The K-M, ROC, and DCA curves all validated the fine predictive performance of our prognostic signature. We also revealed the significant clinical value of each signature in PRAD. The enrichment analysis suggested the correlation of these genes with the calcium signaling pathway, Transforming Growth Factor Beta 1 (TGF-β), and Wingless-Type MMTV Integration Site Family (WNT) pathways, implying that these genes might be involved in the migration of PRAD. In conclusion, the 6-gene ferroptosis-related signature could serve as a novel biomarker for predicting the prognosis in PRAD. Their function in cancer migration needs further investigation.

Keywords

Prostate cancer; Ferroptosis; Risk model; Prognosis

1. Introduction

Prostate adenocarcinoma (PRAD) is a kind of frequently diagnosed cancer in men in many countries, especially in Europe, Australia and America [1]. Although the molarity of PRAD decreased over several years, its molarity is still high in the world [1]. At present, at least 20% of patients diagnosed with PRAD and undergone radical prostatectomy, brachytherapy or other therapies may experience biochemical recurrence during the follow-up period [2–4]. Early diagnosis and treatment could reduce mortality rates in patients diagnosed with PRAD [5], but most patients were diagnosed with advanced or metastatic PRAD because of the uncommon screening [6]. Thus, it is imperative to identify new biomarkers and establish the prognosis model.

Recently, some studies showed that ferroptosis could inhibit the cell proliferation to regulate the progression of cancers [7], including PRAD [8]. Ferroptosis is an iron ion-induced cell death which is varied from other programmed cell death including apoptosis, cell necrosis, autophagy, and their different characteristics was presented in the aspect of morphology, biochemistry and genetics [9, 10]. Some studies revealed that ferroptosis was correlated to the increasing content of peroxidation of phospholipids and reactive oxygen species (ROS), which were mainly regulated by Glutathione peroxidase (GPX4) and solute carrier family 7 member 11 (SLC7A11) [9]. In many cancers, erastin and RAS-selective lethal 3 (RSL3) showed a promising anti-cancer activity, because they could respectively decrease the expression of SLC7A11 and GPX4 [11, 12]. Ghoochani *et al.* [9] identified that erastin and RSL3 inhibited tumor growth *in vivo* and cell migration *in vitro*. Besides, Bordini *et al.* [13] claimed that the PRAD cells with high iron sensitivity could result in cell membrane protein damage. On the other hand, Butler *et al.* [14] demonstrated that down-regulation of 2,4-Dienoyl-CoA Reductase 1 (DECR1) in PRAD cells could suppress

the proliferation and migration of cells through increasing the content of cellular polyunsaturated fatty acids to enhance mitochondrial oxidative stress and lipid peroxidation, which eventually caused the promotion of ferroptosis. These results suggested that ferroptosis play a vital role in the development and prognosis in PRAD.

At present, the signatures and risk model based on ferroptosis related genes (FRGs) were widely applied in the prediction of many cancers [15–17]. Moreover, these models showed a great prediction value. Thus, in our study, we aimed to screen out FRGs and established a prognosis model to predict the progression free interval (PFI) of PRAD. Furthermore, we explore the potential molecule mechanism of each signature. This study provided useful biomarkers for PRAD and revealed the possible pathogenic mechanism, which laid the foundation for further research.

2. Methods

2.1 Data collection

The gene expression profile and corresponding clinical information of patients diagnosed with PRAD were collected from The Cancer Genome Atlas (TCGA, https://www.cancer.gov/about-nci/organization/ccg/research/structural-genomics/tcga). Additionally, 64 FRGs were collected from PathCard.

2.2 The identification of FRGs

We assessed the difference in expression of 64 FRGs in the PRAD samples compared with the normal samples through the R package *t*.test function, and the p.adjust function was applied to determine the false discovery rate (FDR) of each gene. FRGs with p-value < 0.05 were enrolled in the further analyses.

2.3 Construction of prediction model based on FRGs

Firstly, we executed univariate Cox analysis to determine FRGs which were significantly related to the progression-free interval (PFI) time by R package survival. Then, we integrated the PFI time, status and expression, and executed the Lasso regression analysis with the R package glmnet. Subsequently, we conducted the multivariate Cox regression analysis to filter genes which could independently predict the prognosis. Based on the Cox coefficient and gene expression value, we build a prediction model.

2.4 Performance assessment of the prediction model

The receiver operating characteristic (ROC) is a typical method for the validation of the prognosis model. We performed the ROC analysis to explore the performance of our risk model for predicting survival by using R package pROC (version 1.17.0.1), then area under the curve (AUC) and the confidence interval were evaluated by using ci function of pROC. Additionally, we also used decision curve analysis (DCA) to assess the performance of our prognosis model by R package ggDCA.

2.5 Single-sample gene set enrichment analysis (ssGSEA)

We obtained the c2.cp.kegg.v7.4.symbols.gmt subset from the molecular signatures database (www.gsea-msigdb.org/gsea/downloads.jsp) to calculate the activity score of 187 Kyoto Encyclopedia of Genes and Genomes (KEGG) pathways by Single-sample gene set enrichment analysis (ssGSEA). The minimum gene was set to 5, while the maximum gene was set to 5000. After the enrichment score of each sample in each gene set was calculated, the enrichment score matrix was obtained. Then, we evaluated the relationship between our risk model and the 187 pathway scores by the Pearson method.

2.6 Gene set enrichment analysis (GSEA) on each signature

We also executed the GSEA on each signature within the risk model for exploring the potential mechanism. The gene sets "c5.go.v7.4.symbols" and "c2.cp.kegg.v7.4.symbols" were obtained from the MSigDB database (https://www.gsea-msigdb.org/gsea/msigdb). The R package "clusterProfiler" was used to carry out GSEA.

2.7 Statistical analysis

The statistical analysis was performed in SPSS 25 (IBM Corp., Armonk, NY, USA). For quantitative data, the comparison between the two groups was evaluated by independent sample *t*-test. Log-rank test was applied to assess the survival difference between the 2 groups, and the Pearson test was used for the correlation analysis between 2 quantitative variables. $p < 0.05$ was considered statistically significant.

3. Results

3.1 The expression of FRGs in PRAD

Firstly, we explored the expression of each FRGs in the PRAD group in comparison with the normal group. As can be seen from Fig. 1, 17 FRGs expressions were markedly upregulated, while 24 FRGs expression level were markedly lower in the PRAD group than the control group ($p < 0.05$). Then the 41 genes were enrolled in further analyses.

3.2 Establishment and validation of the risk model

Then, univariate Cox regression analysis was used to filter the significant genes closely correlated with the PFI of patients. As presented in Fig. 2, 16 genes were remarkably correlated with the PFI time of patients diagnosed with PRAD (all $p < 0.05$). In order to filter the more valuable biomarkers, we performed the Lasso regression analysis to remove the redundant genes. It was obvious that the optimal Lasso model was determined when lambda value was 0.04 (Fig. 3A), and 11 genes were screened out by 10-fold cross-validation (Fig. 3B).

Next, the multivariate Cox regression analysis was used to assess the independent prognostic role of signatures in PRAD. The results showed that 6 genes could independently

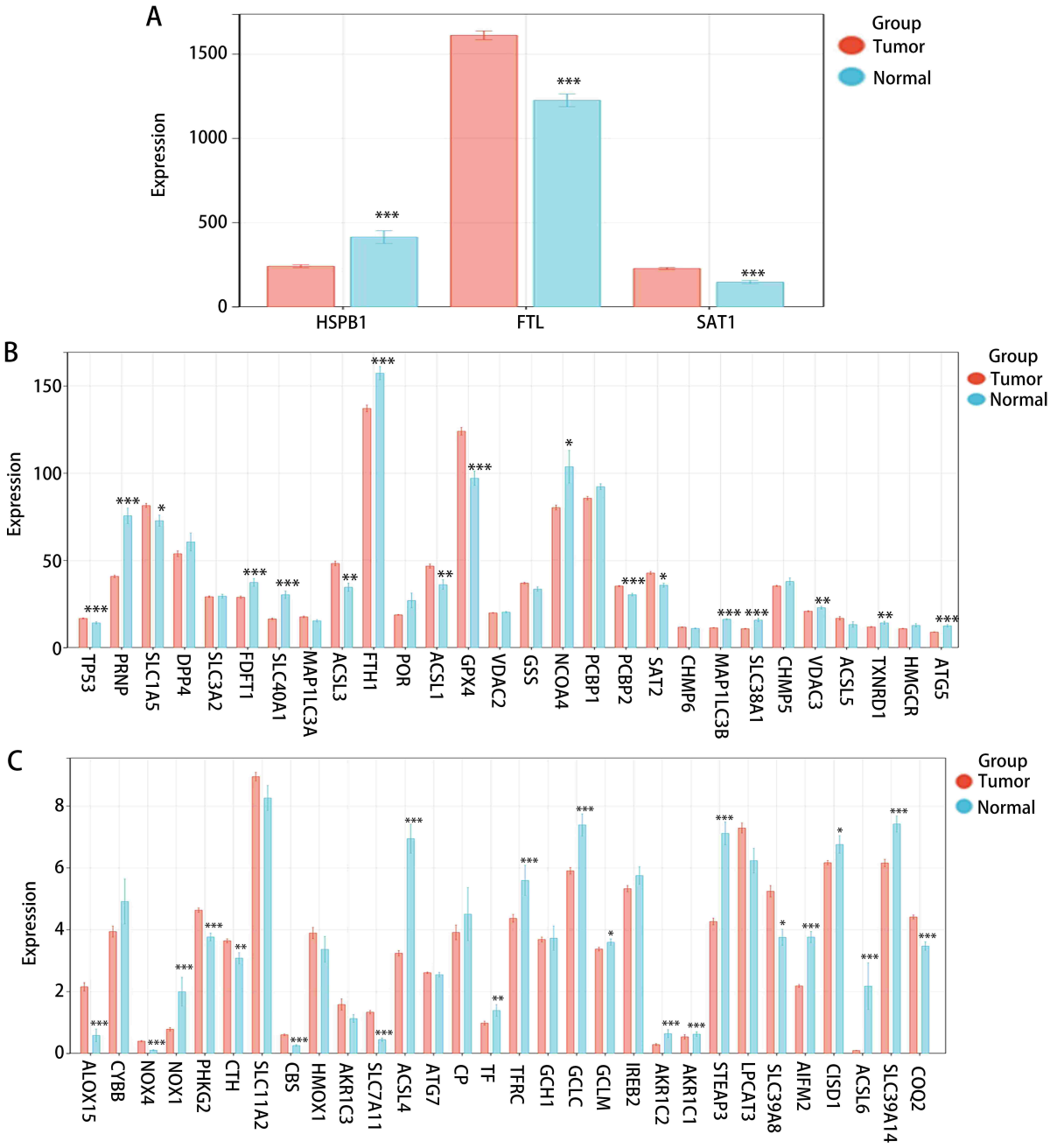

FIGURE 1. The expression of 64 FRGs in tumor and normal tissues. *$p < 0.05$, **$p < 0.01$, ***$p < 0.001$.

predict the prognosis of PRAD, namely TFRC, FTH1, PCBP2, ACSL3, PRNP and LPCAT3 (Table 1). Based on multivariate Cox coefficients and expression value, a risk model was established. The 6-signature risk score = 0.108 × TFRC + 0.007 × FTH1 + 0.026 × PCBP2 − 0.007 × ACSL3 − 0.021 × PRNP − 0.074 × LPCAT3.

After risk scores of all samples were determined, we visualized risk score distribution among all samples (Fig. 3C). It was obvious that the most death was located in high-risk areas, which indicated that this risk model could efficiently distinguish the high and low survival probability of patients with PRAD.

Next, ROC and DCA curves were applied to evaluate our risk model. According to Fig. 4A, the AUC areas of the model were respectively 0.75, 0.74 and 0.68 at 1, 3 and 5 years. Additionally, the DCA curve was used to graphically reveal the clinical utility of the prediction model. As can be seen from Fig. 4B, the prediction model achieved more benefits within a certain range of high risk thresholds. Moreover, the Kaplan-Meier (K-M) curve identified that a low risk score was remarkably associated with a good prognosis in PRAD (Fig. 4C).

Besides, we compared our risk model with other signatures. Li *et al.* [18] constructed a 2-gene signature PFI prediction model. We determined the risk scores of all samples and performed the ROC and DCA based on their risk score (Fig. 4D,E). As shown in Fig. 4D, AUC areas of the 2-gene signature model were respectively 0.68, 0.74 and 0.69 at 1, 3, 5 years. Meanwhile, the results of DCA demonstrated that our prediction model had a greater clinical utility compared with

TABLE 1. Univariate and multivariate Cox regression analysis of 6 genes.

	Univariate		Multivariate	
	HR (95% CI)	*p*-value	HR (95% CI)	*p*-value
TFRC	1.125	3.08×10^{-5}	1.115	2.44×10^{-4}
FTH1	1.008	1.15×10^{-4}	1.007	0.003
PCBP2	1.033	0.019	1.027	0.039
ACSL3	0.991	0.027	1.027	0.015
PRNP	0.985	0.042	0.979	0.004
LPCAT3	0.943	0.043	0.928	0.027

HR: Hazard Ratio; CI: Confidence Interval; TFRC: Transferrin Receptor; FTH1: Ferritin Heavy Chain 1 (FTH1), PCBP2: Poly(RC) Binding Protein 2; ACSL3: Acyl-CoA Synthetase Long Chain Family Member 3; PRNP: Prion Protein; LPCAT3: Lysophosphatidylcholine Acyltransferase 3.

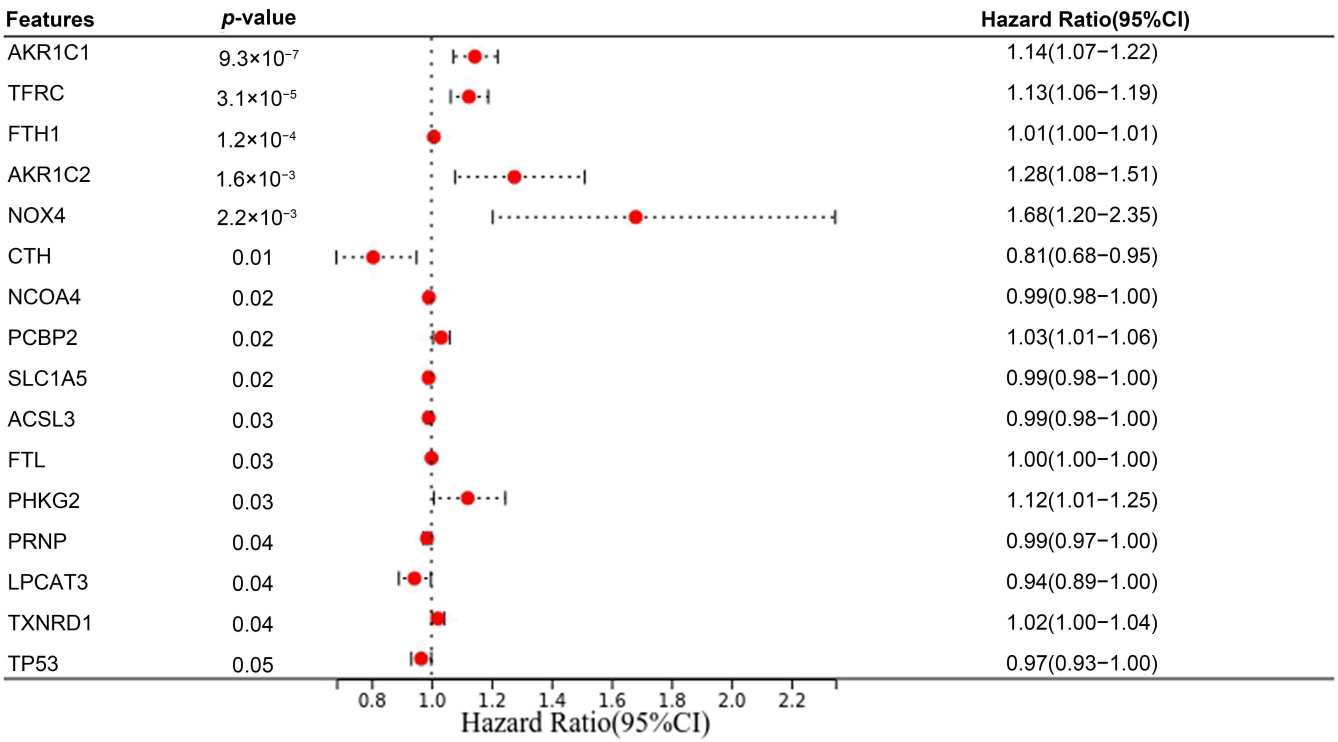

FIGURE 2. Univariate Cox regression analysis on 41 FRGs.

the 2-gene signature model. Additionally, the low risk score group also showed better prognosis than high risk score group in 2-gene signature model (Fig. 4F). The results supported the favorable prediction performance of our 6-gene model.

3.3 Correlation of risk score with clinical characteristics

Besides, we assessed the correlation between clinical characteristics and risk scores. According to Fig. 5A–F, the risk score was intimately correlated with clinical characteristics. The risk score was evidently increased in the older (age ≥60), T3 + T4, N1 and M1 groups in contrast to the younger (age <60), T1 + T2, N0, M0 groups. Besides, in the aspect of residual tumor, the risk score was observably lower in R1 stage than R0 stage, followed by an obvious decrease in the R2 stage in comparison with the R1 stage ($p < 0.05$). Furthermore, the risk score was higher in the patients with the number of lymphnodes more than 15 compared with the patients with the number of lymphnodes less than 15.

3.4 Potential mechanism exploration

To unveil the relationship between the risk score and biological pathway, we first calculated the ssGSEA scores of every PRAD sample according to the gene expression profile. Then, we determined the correlation between risk score and biological pathway. From Fig. 6, it was obvious that risk score was evidently and negatively related to propanoate metabolism, lysine degradation, long term depression, adherens junction, vasopressin regulated water reabsorption, long term potentiation, gap junction and valine leucine and isoleucine degradation, while risk score was evidently and positively related base excision repair and DNA replication, which indicated that these pathways were closely related to tumor development.

We further explored the detailed function of each signature

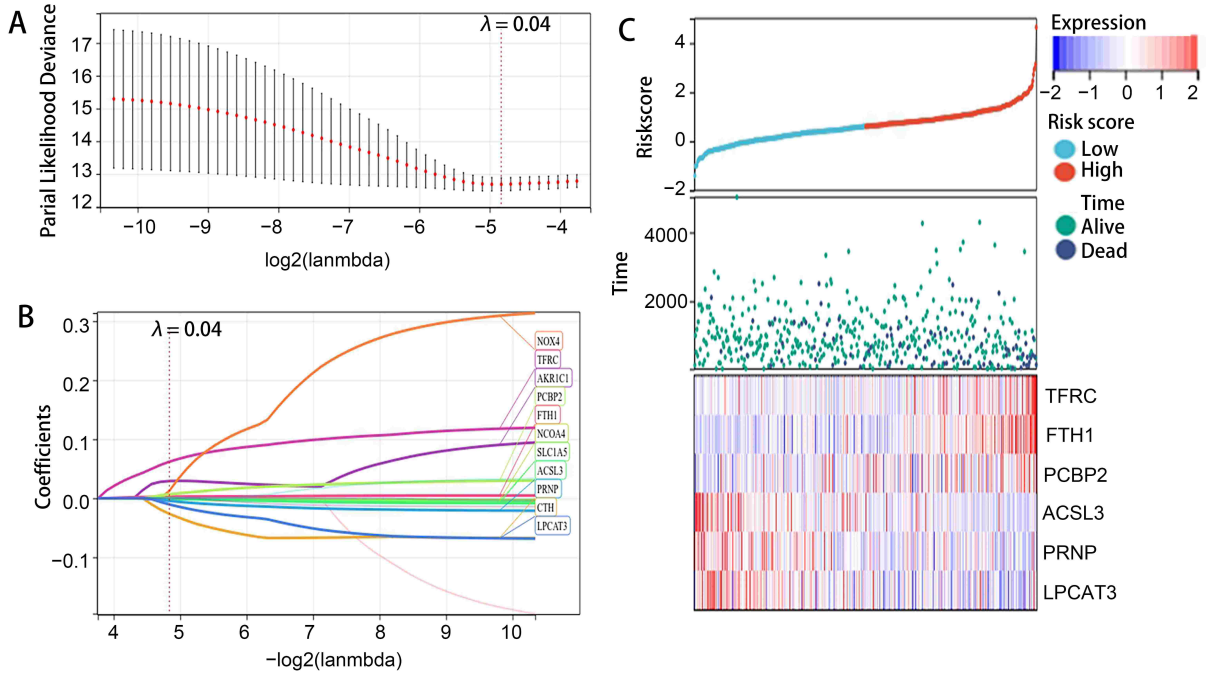

FIGURE 3. Lasso analysis of FRGs. (A) The lambda value and corresponding partial likelihood values for the prognosis model. (B) 11 FRGs were screened out in the optimal lambda. (C) Distribution of risk score, survival status and the expression of the 6 genes.

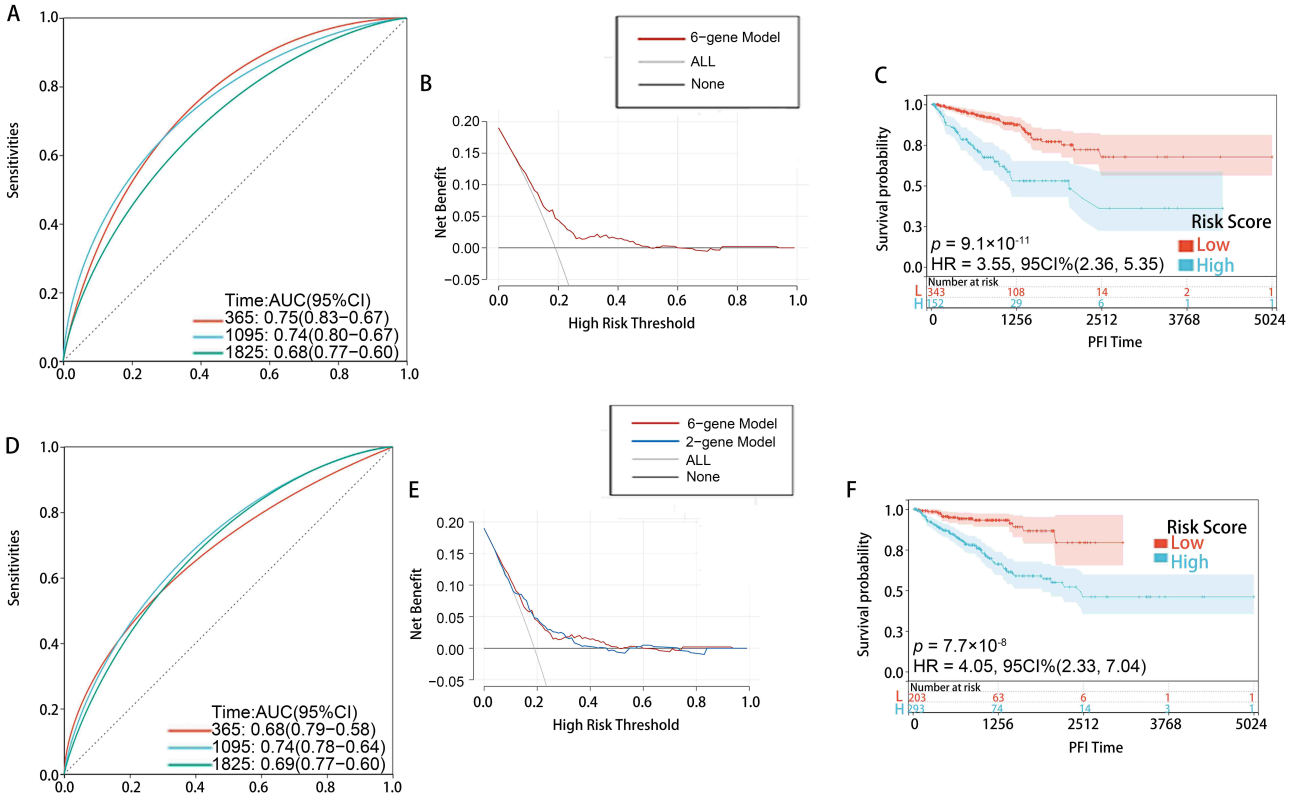

FIGURE 4. The validation and comparison of the 6-signature prediction model. (A) The ROC curves of the 6-signature prediction model. (B) The DCA curves of the 6-signature prediction model. (C) The correlation of risk score and prognosis status in the 6-gene signature prediction model. (D) The ROC curves of the 2-gene signature prediction model. (E) The DCA curves of the 2-gene signature prediction model. (F) The correlation of risk score and prognosis status in the 2-gene signature prediction model.

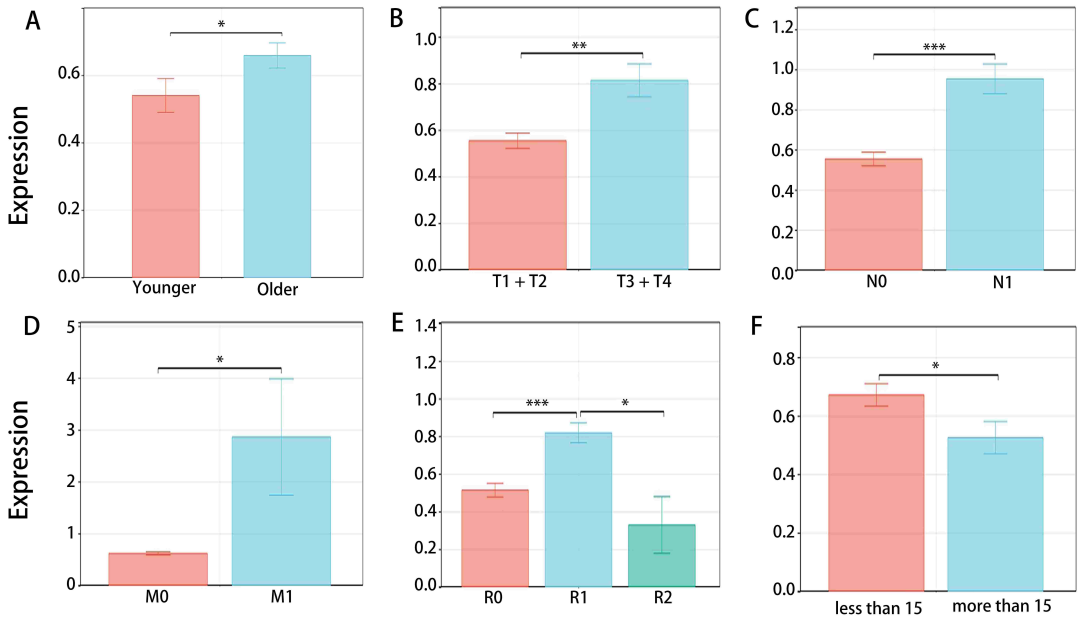

FIGURE 5. The correlation between clinical characteristics and risk score. (A) age. (B) T stage. (C) N stage. (D) M stage. (E) residual tumor. (F) number of lymphnodes. Younger indicated the age <60, and older indicated age ≥60.

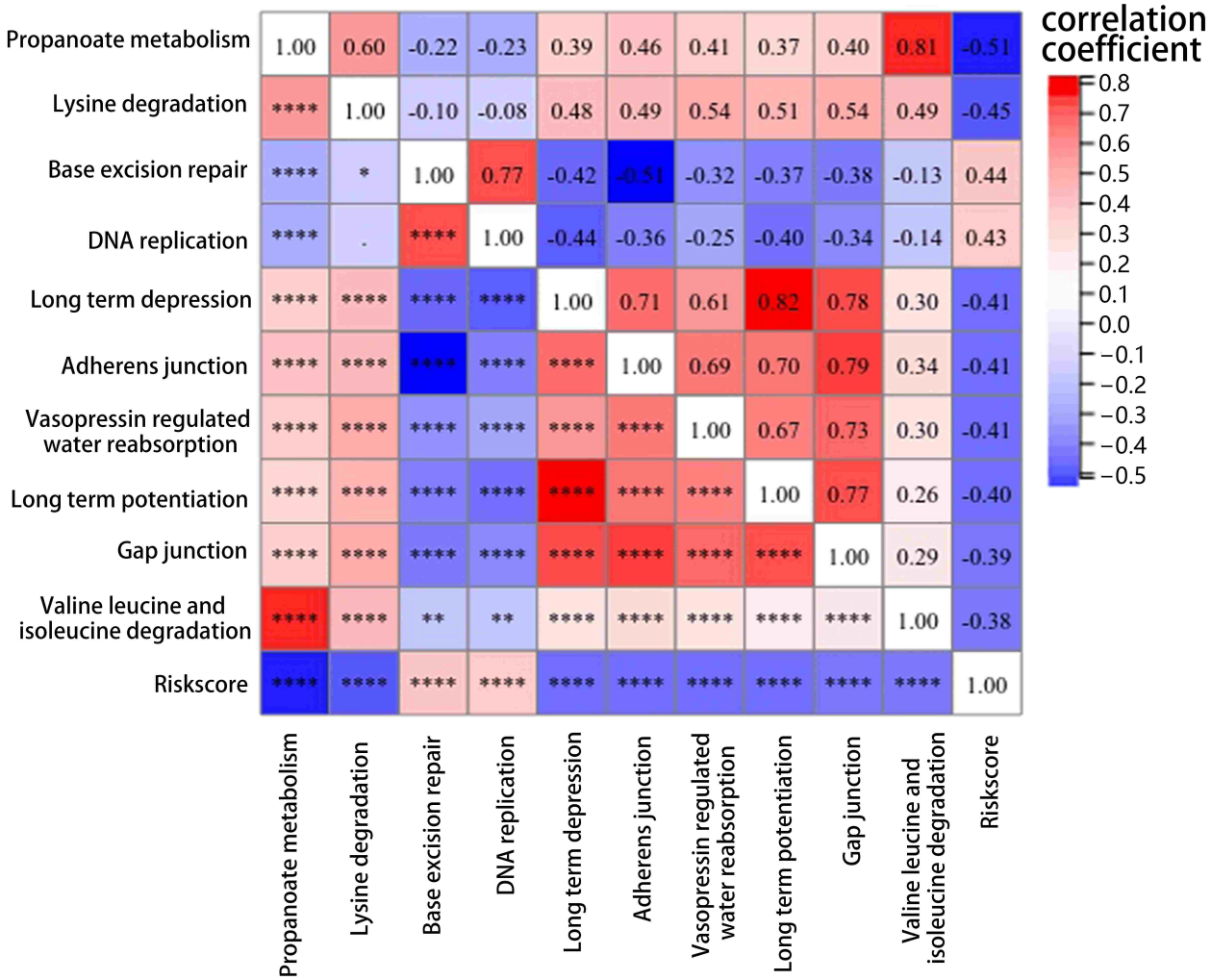

FIGURE 6. The correlation between risk score and KEGG pathways. *$p < 0.05$, **$p < 0.01$, ***$p < 0.001$, ****$p < 0.001$.

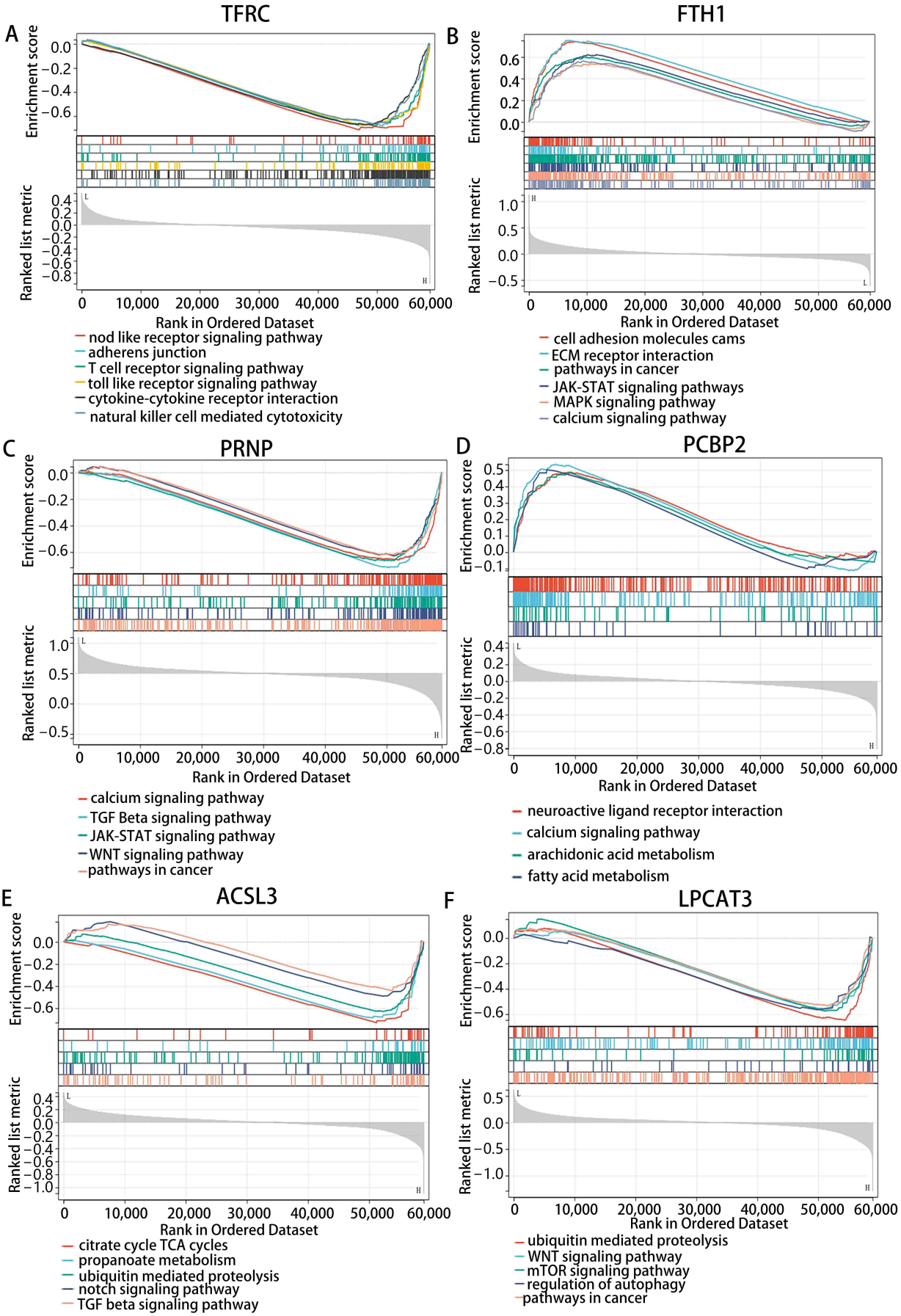

FIGURE 7. The enriched pathway analysis by GSEA in PRAD. (A) TFRC. (B) FTH1. (C) PRNP. (D) PCBP2. (E) ACSL3. (F) LPCAT3.

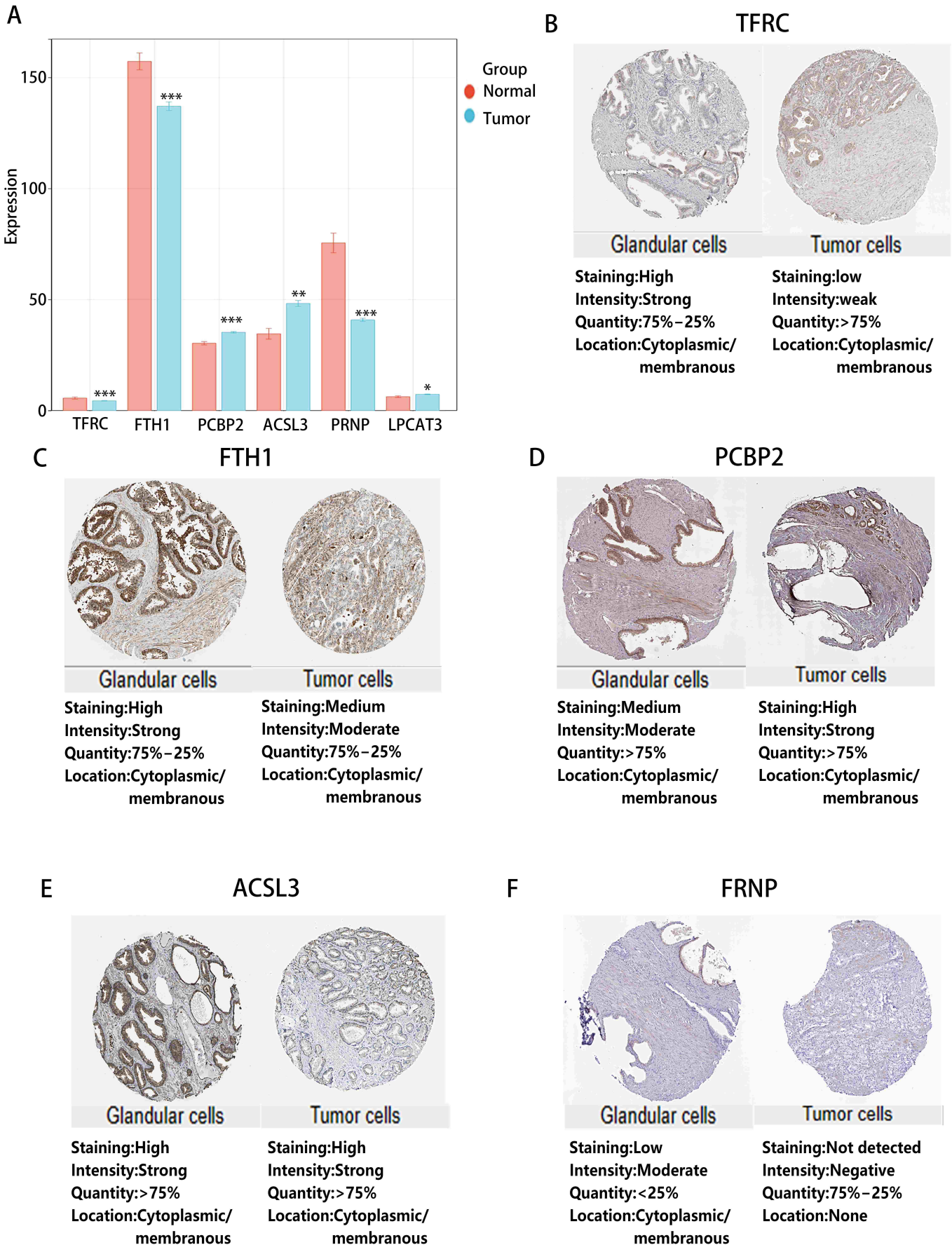

FIGURE 8. The expression and prognostic value analyses of each signature. (A) The expression of 6 signatures in the PRAD group in comparison with the normal group. (B–F) The protein level of signatures in PRAD.

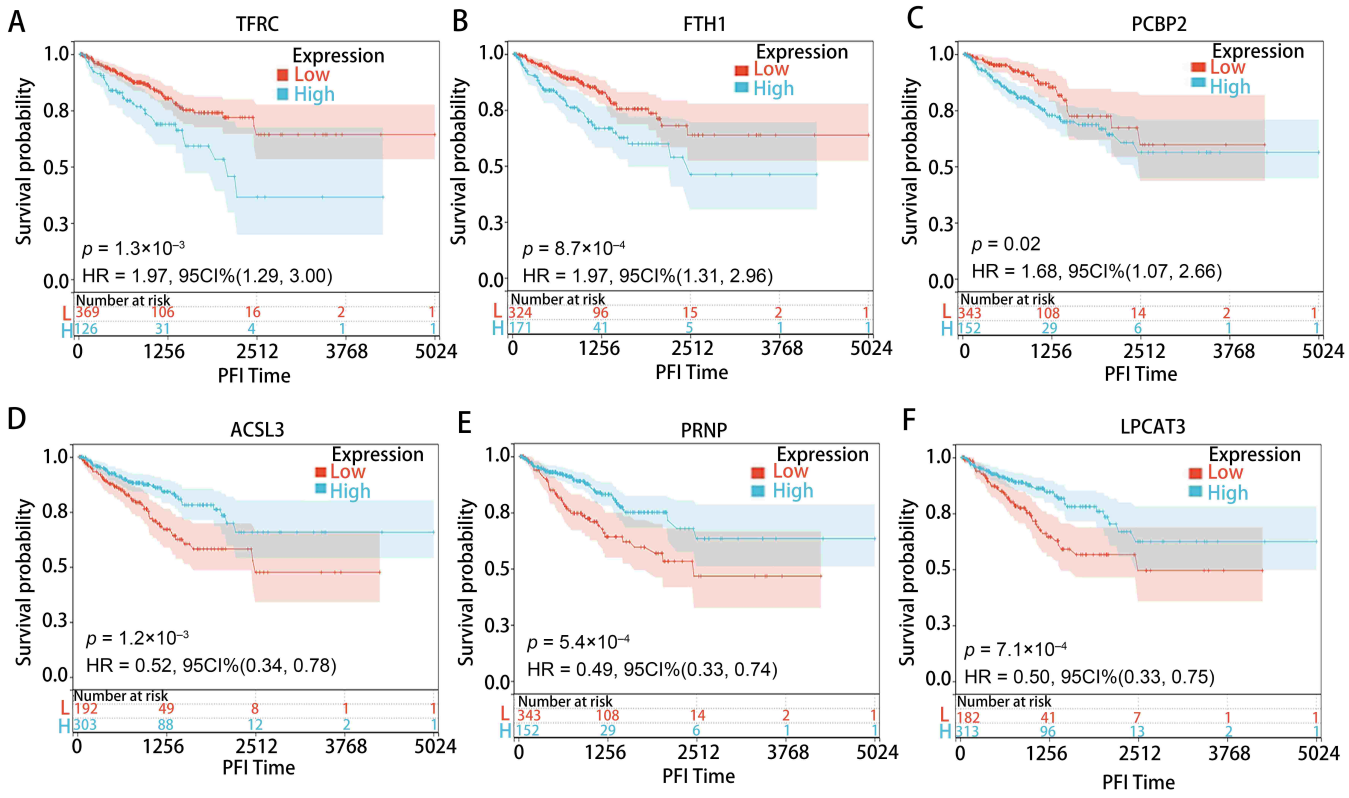

FIGURE 9. The prognostic value analyses of each signature in the PFI of PRAD. (A–F) The correlation between the expression of every signature, namely TFRC, FTH1, PCBP2, ACSL3, PRNP and LPCAT3, and PFI in patients with PRAD.

in PRAD by GSEA. The significantly enriched pathways were shown in Fig. 7A–F. It followed that most pathways were positively related to the risk score, such as cell adhesion molecules cams, calcium signaling pathway and transforming growth factor (TGF) beta signaling pathway, which could promote the development of tumors. It indicated that the imbalance of these pathways was intimately associated with cancer development.

3.5 The expression and potential clinical value of 6 signatures in PRAD

As presented in Fig. 8A, TFRC, FTH1 and PRNP were significantly downregulated, while PCBP2, ACSL3 and LPCAT3 were significantly upregulated in PRAD in comparison with the normal group ($p < 0.05$). Although the protein levels of LPCAT3 were not detected in The Human Protein Atlas (HPA), the abnormal protein levels of other genes were similar in tumor and normal tissues (Fig. 8B–F). Survival analysis (Fig. 9A–C) identified that high expressions of TFRC, FTH1 and PCBP2 were closely correlated with poor prognosis. On the contrary, the low expressions of ACSL3, PRNP and LPCAT3 were closely related to the poor prognosis (Fig. 9D–F).

4. Discussion

Ferroptosis is an iron-dependent form of regulated cell death, which is induced by the toxic build-up of lipid peroxides on cellular membranes [19]. Because of the unique mechanism and morphology, most researches attached importance to ferroptosis in tumor research recently. In this study, we detected significant ferroptosis-related signatures related to the prognosis of PRAD and established a 6-gene risk model. The ROC, DCA and K-M analyses demonstrated the favorable performance of the 6-gene model for predicting the prognosis. Subsequently, we explored the detailed function of each signature within the model.

TFRC (transferrin receptor) is an important participant in intracellular iron transport [20]. The study has indicated that yes-associated protein (YAP) can increase the iron content in hepatocellular carcinoma cell by upregulating expression of TFRC resulted from O-GlcNAcylation [21]. Huang *et al.* [22] found that TFRC promoted the epithelial ovarian cancer cell proliferation and metastasis. Besides, it also revealed that high TFRC expression was negatively associated with the immune-related pathways, which implied the risk of tumor immune escape and migration. Down-regulation of FTH1 (ferritin heavy chain 1) has been found to be a key determinant for baicalin-induced ferroptosis [23]. Ali *et al.* [24] found that FTH1 exerted significant antigrowth effects in breast cancer. We identified that upregulated expression of FTH1 was related to the poor prognosis, which may be contributed to the regulation of the classically activated macrophages (CAMs) and extracellular matrix (ECM). Besides, high expression of PRNP (prion protein) predicted a poor prognosis of gastric cancer [25]. However, Hu *et al.* [26] found that down-regulated PRNP facilitated the proliferation and invasion of ovarian cancer cells. This study identified that PRNP high expression was favorable to the prognosis of PRAD, which may be associated with the inhibition of the migration-related pathways.

For PCBP2 (bind poly (rC) binding protein 2), previous

studies had demonstrated its oncogenic role in glioma [27], gastric cancer [28], and pancreatic cancer [29]. This study also confirmed its unfavorable prognostic impact in PARD. Pathway analysis found that PCBP2 high expression activated the calcium signaling pathway and fatty acid metabolism, which also suggested the risk of cancer migration. ACSL3 (acyl-CoA synthetase long-chain 3) is an androgen-responsive gene and previous studies revealed ACSL3 expression was upregulated in a variety of cancers [30]. In our study, high expression of ACSL3 was associated with a better prognosis of PRAD, which may be associated with the inhibition of the tricarboxylic acid (TCA) cycle and migration-related pathways. LPCAT3 (Lysophosphatidylcholine acyltransferase 3) is regulated by the liver X receptor and have a vital effect on lipoprotein production [31]. Ke *et al.* [32] had indicated that LPCAT3 could effectively predict the prognosis of acute myeloid leukemia and related to ferroptosis. In this study, patients with high expression of LPCAT3 had a better prognosis, which may be related to the inhibition of cancer-related pathways.

These researches have confirmed the importance of the 6 signatures selected in this study. All the signatures were significantly correlated with the migration-related pathways. The detailed regulation of these signatures in the progression of PRAD needs further investigation.

5. Conclusions

We determined 41 differentially expressed FRGs between PRAD and normal tissues. Based on the further univariable Cox regression, Lasso, and multivariable Cox regression analyses, a 6-signature model was finally constructed for prediction of PFI in PRAD. We then confirmed the favorable prediction performance of our risk model by ROC, DCA, and K-M analysis. The pathway enrichment analyses implied that the 6 signatures might be engaged in the migration of cancer cells. This study provided the significant biomarkers for PRAD, and the detailed function in PRAD progression needs further verification.

AVAILABILITY OF DATA AND MATERIALS

The dataset used and/or analyzed during the current study is available from the corresponding author on reasonable request.

AUTHOR CONTRIBUTIONS

JJG—Conception and design; ZMP—Collection and assembly of data; GAZ—Data analysis and interpretation. All authors—Manuscript writing, read and approved the final manuscript.

ETHICS APPROVAL AND CONSENT TO PARTICIPATE

Not applicable.

ACKNOWLEDGMENT

Not applicable.

FUNDING

This research received no external funding.

CONFLICT OF INTEREST

The authors declare no conflict of interest.

REFERENCES

[1] Sung H, Ferlay J, Siegel RL, Laversanne M, Soerjomataram I, Jemal A, *et al*. Global Cancer Statistics 2020: GLOBOCAN estimates of incidence and mortality worldwide for 36 cancers in 185 countries. CA: A Cancer Journal for Clinicians. 2021; 71: 209–249.

[2] Brockman JA, Alanee S, Vickers AJ, Scardino PT, Wood DP, Kibel AS, *et al*. Nomogram predicting prostate cancer-specific mortality for men with biochemical recurrence after radical prostatectomy. European Urology. 2015; 67: 1160–1167.

[3] Van den Broeck T, van den Bergh RCN, Arfi N, Gross T, Moris L, Briers E, *et al*. Prognostic value of biochemical recurrence following treatment with curative intent for prostate cancer: a systematic review. European Urology. 2019; 75: 967–987.

[4] Venclovas Z, Jievaltas M, Milonas D. Significance of time until PSA recurrence after radical prostatectomy without neo- or adjuvant treatment to clinical progression and cancer-related death in high-risk prostate cancer patients. Frontiers in Oncology. 2019; 9: 1286.

[5] Nunes SBR, de Matos Oliveira F, Neves AF, Araujo GR, Marangoni K, Goulart LR, *et al*. Association of vitamin D receptor variants with clinical parameters in prostate cancer. SpringerPlus. 2016; 5: 364.

[6] Liu Z, Zhong J, Cai C, Lu J, Wu W, Zeng G. Immune-related biomarker risk score predicts prognosis in prostate cancer. Aging. 2020; 12: 22776–22793.

[7] Wang Y, Wei Z, Pan K, Li J, Chen Q. The function and mechanism of ferroptosis in cancer. Apoptosis. 2020; 25: 786–798.

[8] Lv Z, Wang J, Wang X, Mo M, Tang G, Xu H, *et al*. Identifying a ferroptosis-related gene signature for predicting biochemical recurrence of prostate cancer. Frontiers in Cell and Developmental Biology. 2021; 9: 666025.

[9] Ghoochani A, Hsu E, Aslan M, Rice MA, Nguyen HM, Brooks JD, *et al*. Ferroptosis inducers are a novel therapeutic approach for advanced prostate cancer. Cancer Research. 2021; 81: 1583–1594.

[10] Stockwell BR, Friedmann Angeli JP, Bayir H, Bush AI, Conrad M, Dixon SJ, *et al*. Ferroptosis: a regulated cell death nexus linking metabolism, redox biology, and disease. Cell. 2017; 171: 273–285.

[11] Hangauer MJ, Viswanathan VS, Ryan MJ, Bole D, Eaton JK, Matov A, *et al*. Drug-tolerant persister cancer cells are vulnerable to GPX4 inhibition. Nature. 2017; 551: 247–250.

[12] Viswanathan VS, Ryan MJ, Dhruv HD, Gill S, Eichhoff OM, Seashore-Ludlow B, *et al*. Dependency of a therapy-resistant state of cancer cells on a lipid peroxidase pathway. Nature. 2017; 547: 453–457.

[13] Bordini J, Morisi F, Elia AR, Santambrogio P, Pagani A, Cucchiara V, *et al*. Iron induces cell death and strengthens the efficacy of antiandrogen therapy in prostate cancer models. Clinical Cancer Research. 2020; 26: 6387–6398.

[14] Nassar ZD, Mah CY, Dehairs J, Burvenich IJ, Irani S, Centenera MM, *et al*. Human DECR1 is an androgen-repressed survival factor that regulates PUFA oxidation to protect prostate tumor cells from ferroptosis. Elife. 2020; 9: e54166.

[15] Liang JY, Wang DS, Lin HC, Chen XX, Yang H, Zheng Y, *et al*. A novel ferroptosis-related gene signature for overall survival prediction in patients with hepatocellular carcinoma. International Journal of Biological Sciences. 2020; 16: 2430–2441.

[16] Lu T, Xu R, Li Q, Zhao J, Peng B, Zhang H, *et al*. Systematic profiling of ferroptosis gene signatures predicts prognostic factors in esophageal squamous cell carcinoma. Molecular Therapy Oncolytics. 2021; 21: 134–143.

[17] Wang D, Wei G, Ma J, Cheng S, Jia L, Song X, *et al*. Identification of

the prognostic value of ferroptosis-related gene signature in breast cancer patients. BMC Cancer. 2021; 21: 645.

[18] Li S, Shi L, Li F, Yao B, Chang L, Lu H, *et al*. Establishment of a novel combined nomogram for predicting the risk of progression related to castration resistance in patients with prostate cancer. Frontiers in Genetics. 2022; 13: 823716.

[19] Lei G, Zhuang L, Gan B. Targeting ferroptosis as a vulnerability in cancer. Nature Reviews Cancer. 2022; 22: 381–396.

[20] Yang C, Li J, Guo Y, Gan D, Zhang C, Wang R, *et al*. Role of TFRC as a novel prognostic biomarker and in immunotherapy for pancreatic carcinoma. Frontiers in Molecular Biosciences. 2022; 9: 756895.

[21] Zhu G, Murshed A, Li H, Ma J, Zhen N, Ding M, *et al*. O-GlcNAcylation enhances sensitivity to RSL3-induced ferroptosis *via* the YAP/TFRC pathway in liver cancer. Cell Death Discovery. 2021; 7: 83.

[22] Huang Y, Huang J, Huang Y, Gan L, Long L, Pu A, *et al*. TFRC promotes epithelial ovarian cancer cell proliferation and metastasis *via* up-regulation of AXIN2 expression. American Journal of Cancer Research. 2020; 10: 131–147.

[23] Kong N, Chen X, Feng J, Duan T, Liu S, Sun X, *et al*. Baicalin induces ferroptosis in bladder cancer cells by downregulating FTH1. Acta Pharmaceutica Sinica B. 2021; 11: 4045–4054.

[24] Ali A, Shafarin J, Abu Jabal R, Aljabi N, Hamad M, Sualeh Muhammad J, *et al*. Ferritin heavy chain (FTH1) exerts significant antigrowth effects in breast cancer cells by inhibiting the expression of c-MYC. FEBS Open Bio. 2021; 11: 3101–3114.

[25] Choi M, Moon S, Eom HJ, Lim SM, Kim YH, Nam S. High expression of PRNP predicts poor prognosis in korean patients with gastric cancer. Cancers. 2022; 14: 3173.

[26] Hu K, Zhang X, Zhou L, Li J. Downregulated PRNP facilitates cell proliferation and invasion and has effect on the immune regulation in ovarian cancer. Journal of Immunology Research. 2022; 2022: 1–11.

[27] Mao J, Sun Z, Cui Y, Du N, Guo H, Wei J, *et al*. PCBP2 promotes the development of glioma by regulating FHL3/TGF-β/Smad signaling pathway. Journal of Cellular Physiology. 2020; 235: 3280–3291.

[28] Chen C, Lei J, Zheng Q, Tan S, Ding K, Yu C. Poly(rC) binding protein 2 (PCBP2) promotes the viability of human gastric cancer cells by regulating CDK2. FEBS Open Bio. 2018; 8: 764–773.

[29] Li Y, Zhao Z, Lin C, Liu Y, Staveley-OCarroll KF, Li G, *et al*. Silencing PCBP2 normalizes desmoplastic stroma and improves the antitumor activity of chemotherapy in pancreatic cancer. Theranostics. 2021; 11: 2182–2200.

[30] Quan J, Bode AM, Luo X. ACSL family: the regulatory mechanisms and therapeutic implications in cancer. European Journal of Pharmacology. 2021; 909: 174397.

[31] Shao G, Qian Y, Lu L, Liu Y, Wu T, Ji G, *et al*. Research progress in the role and mechanism of LPCAT3 in metabolic related diseases and cancer. Journal of Cancer. 2022; 13: 2430–2439.

[32] Ke P, Bao X, Liu C, Zhou B, Huo M, Chen Y, *et al*. LPCAT3 is a potential prognostic biomarker and may be correlated with immune infiltration and ferroptosis in acute myeloid leukemia: a pan-cancer analysis. Translational Cancer Research. 2022; 11: 3491–3505.

How to cite this article: Jing-jing Guan, Zhou-min Pan, Guan-an Zhao. Identification of a 6-gene signature associated with ferroptosis for predicting the prognosis in prostate cancer. Journal of Men's Health. 2023; 19(2): 58-68. doi: 10.22514/jomh.2023.013.